Elevated CO2 alters nitrogen cycle in global croplands

Jinglan Cui
Zhejiang University
Xiuming Zhang
Zhejiang University
Stefan Reis
UK Centre for Ecology & Hydrology https://orcid.org/0000-0003-2428-8320
Chen Wang
Zhejiang University
Sitong Wang
Zhejiang University
Peiying He
Zhejiang University
Hongyi Chen
Zhejiang University
Hans van Grinsven
PBL Netherlands Environmental Assessment Agency https://orcid.org/0000-0001-7304-0706
Baojing Gu (bjgu@zju.edu.cn)
Zhejiang University https://orcid.org/0000-0003-3986-3519

Article

Keywords:

Posted Date: January 26th, 2023

DOI: https://doi.org/10.21203/rs.3.rs-2439666/v1

Additional Declarations: There is **NO** Competing Interest.

Version of Record: A version of this preprint was published at Nature Sustainability on June 22nd, 2023. See the published version at https://doi.org/10.1038/s41893-023-01154-0.

Elevated CO_2 alters nitrogen cycle in global croplands

Jinglan Cui[1,2], Xiuming Zhang[1], Stefan Reis[3,4,5], Chen Wang[1], Sitong Wang[1], Peiying He[1], Hongyi Chen[1], Hans van Grinsven[6], Baojing Gu[1,2,7*]

[1]College of Environmental and Resource Sciences, Zhejiang University, Hangzhou, 310058, China.
[2]Policy Simulation Laboratory, Zhejiang University, Hangzhou, 310058, China.
[3]UK Centre for Ecology & Hydrology, Bush Estate, Penicuik, Midlothian, EH26 0QB, UK.
[4]University of Exeter Medical School, European Centre for Environment and Health, Knowledge Spa, Truro, TR1 3HD, UK.
[5]The University of Edinburgh, School of Chemistry, Level 3, Murchison House, 10 Max Born Crescent, The King's Buildings, West Mains Road, Edinburgh EH9 3BF, United Kingdom
[6]PBL Netherlands Environmental Assessment Agency, PO BOX 30314, 2500 GH Hague, Netherlands.
[7]Zhejiang Provincial Key Laboratory of Agricultural Resources and Environment, Zhejiang University, Hangzhou, 310058, China.

* bjgu@zju.edu.cn (B.G.)

Croplands support global food security and human nutrition, representing the largest nitrogen flows globally. Elevated atmospheric carbon dioxide (CO_2) level is a key driver of climate change with multiple impacts on food security, environmental and human health. However, our understanding of how the cropland nitrogen cycle will respond to elevated CO_2, so far is not well developed. We demonstrate that elevated CO_2 alone would induce a synergistic intensification of the nitrogen and carbon cycles, promote nitrogen use efficiency by 19% (14-26%) and biological nitrogen fixation by 55% (28-85%) in global croplands. This would lead to increased crop nitrogen harvest (+12 Tg), substantially lower fertilizer input requirements (-34 Tg) and an overall decline in reactive nitrogen loss (-46 Tg) annually under future elevated CO_2 scenarios by 2050. The impact of elevated atmospheric CO_2 on altered cropland nitrogen cycle would amount to 672 billion US dollars benefit in terms of avoiding damages to human and ecosystem health. Regionally, the largest alteration would materialize in China, India, North America, and Europe. To improve the policy design for food security and sustainable development, it would be paramount to integrate the effect of rising CO_2 on nitrogen cycle into state-of-the-art Earth System Models.

Cropland is the major ecosystem supporting food security and human health with the largest nitrogen flux on Earth[1,2]. Climate change, associated with a continued rise in greenhouse gas emissions, could increase the vulnerability of croplands and threaten global food security[3]. Atmospheric levels of CO_2 have increased by 47% since the Industrial Revolution, reaching an unprecedented level in at least two million years and continuing to exceed 600~1000 ppm by the end of the 21st century[4]. As the primary greenhouse gas, CO_2 also acts as a gaseous fertilizer stimulating plant photosynthesis and productivity, and elevated CO_2 (eCO_2, also known as CO_2 fertilization, CO_2 enrichment) accordingly enhances carbon (C) sequestration in the terrestrial biosphere[5,6]. Meanwhile, nitrogen (N) is a vital element to constitute protein in flora and fauna, and the capability of carbon sequestration in the biosphere is largely limited by N availability[7]. In contrast to extensive studies on the response of C cycle (i.e., net primary productivity, soil organic C) to climate change[8,9], much less emphasis has been placed so far on the response of the N cycle to climate change. Yet, the N cycle will critically determine the potential C sinks or sources in croplands under elevated CO_2 levels, hence it is vital that the coupling relationship between the two crucial biogeochemical cycles, N & C, are better understood[10]. Furthermore, excessive reactive N (N_r, all N forms other than dinitrogen – N_2) use in agriculture has led to adverse impacts on ecosystem and human health, ranging from eutrophication, acidification, air pollution ($PM_{2.5}$) and biodiversity loss[11,12]. Forecast changes in future precipitation regimes are expected to exacerbate N_r runoff and intensify regional eutrophication[13]. Whether the effects of other aspects of climate change, including that of elevated atmospheric CO_2 levels on N_r emissions, have not been well quantified to date.

The climate impact on cropland driven by warming and extreme climate has been highlighted, whereas CO_2 fertilization with its interaction effect is rarely considered in future projection[14,15]. Historic data and experiments reveal that CO_2 fertilization offsets some negative climate impacts on crop production[6,16]. Future high levels of atmospheric CO_2 might increase the optimal temperature of photosynthesis and suppress evapotranspiration with lower stomatal conductance, likely interacting with warming and drought to induce cascade effects[6]. The emerging evidence of large-scale declines in N availability in terrestrial ecosystems[17] and human dietary protein[18] underlines the rising CO_2 is the main driver of global changes for N cycle. Field manipulation experiments simulating responses to elevated CO_2 levels provide the most useful tools for studying the effects of eCO_2 as a single climate change driver on features of the N cycle. Currently, a holistic quantification of N cycle responses to future elevated CO_2 in global croplands is missing. Responses of the N cycle to elevated CO_2 are likely heterogeneous and regionally variable, thus corresponding changes in food production and impacts on environmental and human health may affect regional development and expand inequalities between countries[19,20]. Filling this knowledge gap is essential to constrain Earth System Models (ESM) which are widely applied for the simulation and projection of potential policy interventions and to inform policy-making for global sustainable development[4,21].

Here we assess the responses of key N and C cycle variables to eCO_2 in croplands based on a global dataset of eCO_2 experiments. Then we project future cropland N budgets at a spatial resolution of 0.5 by 0.5 degree under multiple scenarios utilizing the Coupled Human and Natural Systems (CHANS) model[22,23]. Finally, we undertake an impact assessment to achieve a quantitative monetized valuation of eCO_2 impacts on the ecosystem and human health.

Responses of C and N dynamics to eCO_2

We present a global atlas of eCO_2 simulation experiments in croplands comprising FACE (Free-Air CO_2 Enrichment), OTC (Open-Top Chamber), and GC (Greenhouse & Growth Chamber) sites (Fig. 1A). In total, 1003 response ratios were generated for various crop types, including wheat, rice, maize, soybean, and others. Elevated atmospheric CO_2 levels promote crop yield by 21% (95% CI 18% to 25%) relative to ambient CO_2 level (Fig. 1B), values that are consistent across different manipulation methods and regardless if values are derived from field and chamber studies (Extended Data Fig. 1C). The response sensitivity of yield to CO_2 fertilization varies with crop type and magnitude of manipulation ($\mathit{\Delta}CO_2$) (Extended Data Fig. 1A, Extended Data Fig. 2A). Mean annual temperature and mean annual precipitation also moderate the response ratios for the specific type of crop. Soil respiration, mainly CO_2 emissions from plant roots and soil fauna, increased by 25% (19% to 31%), which is much higher than the increase in soil organic C (SOC) of 6% (2% to 9%) (Fig. 1B). The relatively small change in SOC may be attributed to the large soil C stock. Overall, the simulations show an accelerating C cycling trend in global croplands under CO_2 enrichment conditions, likely a result of stimulated plant productivity (crop yield), gaseous C losses to the atmosphere (soil respiration), and C sequestration in soil (SOC).

The higher C availability could provide substrates for microorganism activities closely associated with N cycling i.e., N-fixing bacteria and denitrifiers[24]. Rates of biological N fixation (BNF) are significantly raised by 55% (28% to 85%) (Fig. 1B), suggesting strengthened capability of symbiotic and free-living N fixation microbes to transform N_2 to inorganic N available for crops in cropland[25]. N mineralization is promoted by 22% (6% to 44%), in correspondence with stimulated soil respiration. Soil nitrous oxide (N_2O) emissions increase by 29% (5% to 65%), mainly as a consequence of enhanced denitrification (+24%, 4% to 57%)[26]. Meanwhile, e CO_2 can facilitate N uptake by plants, leading to 19% (14% to 26%) higher N use efficiency (NUE) in croplands. Higher NUE implies lower N_r loss, including reduced N leaching and runoff to water bodies (NO_3^-, -45%, -76% to -13%), as well as decreased emissions to air of ammonia (NH_3) (-21%; -41% to -1%) and nitrogen oxides (NO_x) (-33%, -50% to -9%).

Foliar C:N ratio increased by 19% (15% to 24%) (Fig. 1B). The soil C:N ratio shows a non-significant response to eCO_2, probably due to the large soil C and N pool. In contrast, N content decreased in grain (-7%: -9% to -5%), leaf (-15%, -18% to -10%) and stem (-10%, -18% to -2%) (Fig. 1B). The decrease in N content could be attributable to the dilution of N in plant tissues due to increased C assimilation and lower investment in Rubisco for photosynthesis[27,28]. Long-term observations indicate a general trend of reduced N availability in forest and grassland ecosystems, driven by eCO_2 since the early 20th century[17]. Similar to the N deficiency in unmanaged ecosystems, declining N content in crop harvest of grain, leaf, and stem in croplands is a result of eCO_2. Although additional mineral fertilizer application usually complements N inputs and creates an N-rich environment in agricultural systems, the preference for N allocation to roots rather than to leaves for acquiring higher N uptake under eCO_2 in plants results in a lower leaf N_r content[29].

Overall, elevated atmospheric CO_2 levels induce synergetic intensification of both C and N cycles in global croplands. Increased C availability under CO_2 enrichment is projected to stimulate the intensification of the N cycle, while enhanced N cycling could in turn alleviate N limitations for C assimilation in global cropland systems. Elevated atmospheric CO_2 levels have recently been found to enhance N cycling through higher N return from litterfall, e.g. stimulating consistent tree growth in Tibetan Plateau forests based on observations over a ten-year period [30]. Our simulations further revealed that the synergistic intensification occurs between the N and C cycles in croplands under eCO_2 level at global scale, and indicated that the thus enhanced N cycle would sustain CO_2 fertilization effects on crop yield.

Spatial changes in N budgets under eCO_2

We estimate changes in global N budgets for cropland utilizing the CHANS model, integrating the responses of N parameters to elevated CO_2 levels to derive annual N flows[22] (see supplementary material). We designed a set of baseline scenarios (no climate change, fixed CO_2 levels) and eCO_2 scenarios for a near future period (2030-2050), based on Shared Socio-economic Pathways (SSPs) and Representative Concentration Pathways (RCPs) (Extended Data Fig. 3). Future atmospheric CO_2 levels in the eCO_2 scenarios are derived from CMIP5 models, for three eCO_2 sub-scenarios (SSP1-RCP1.9 "sustainable society", SSP2-4.5 "business-as-usual", and SSP4-RCP6.0 "stratified society"), relative to three baseline scenarios (SSP1, SSP2, and SSP4)[31]. At global scale, eCO_2 will decrease total N input (-27 Tg N), increase N harvest (+12 Tg N), and reduce N surplus (N_r loss & N_2, -39 Tg N) per year under the eCO_2 SSP2-4.5 scenario ("business-as-usual" scenario) relative to a no-climate-change scenario by 2050 (Fig. 2, Fig 3).

The positive effects of CO_2 fertilization on yield outweigh the negative effects on grain N_r content, ultimately resulting in a net increase of N_r harvested in future eCO_2 scenarios. Under the eCO_2 SSP2-4.5 scenario, a significant increase in N_r harvested will occur in East and South Asia, the Great Lakes region in North America, and southeast Latin America (Fig. 2). These regions are also hotspots for crop production and population density, hence the increasing yield and associated N_r harvest can bring immediate food security benefits, especially for low-income countries with considerable famine issues[32].

Global aggregated NUE is modelled to increase from 47% to 57% by 2050 under the SSP2-4.5 scenario (Fig. 2), albeit with regional heterogeneity. The increase in NUE is projected to exceed 20% in the United States, south and east Latin America, Europe, and western Africa, much higher than the minimum increase in NUE of less than 5% in Central America, the Caribbean, most Asia, and eastern Africa. Although the positive response of NUE to eCO_2 can be moderated by mean annual precipitation, the spatial variation of changes in NUE is closely related to background NUE, marked by a higher relative increase in high-NUE regions, which may increase regional inequality[33]. Improved NUE predominantly drives the substantial reductions of total N_r input and losses.

Total N_r inputs are projected to decline, dominated by lower fertilizer (-34 Tg N) and manure input (-5 Tg N), and reduced atmospheric N_r deposition (-3 Tg N); except that BNF will increase drastically by 15 Tg N per year under eCO_2 SSP2-4.5 scenario in 2050 (Fig. 3). Reductions in N_r inputs will be largest in East and South Asia (India and Eastern China), with moderate reductions modelled for other highly intensified agricultural regions, including central and western Europe (Germany, Czech Republic, France, Italy), central and eastern United States and southern Canada, Argentina, and coastal South Australia (Fig. 2). The increased BNF results from stimulated microbial N-fixing quantity given the enhanced C availability in cropland. The reduced N_r deposition is largely attributable to the lower NH_3 and NO_x emissions from croplands under eCO_2, for the Nr deposition mainly derives from these Nr emissions[34]. The producers would probably reduce the use of anthropogenic Nr input for adaptation to the local soil nutrient condition depending on the changing NUE and other natural Nr input sources[35,36]. The reduction in mineral fertilizer and manure application would as well result in reduced costs for agricultural production in most regions. In contrast, some regions in Brazil, central Africa (Cameroon, Nigeria), and Southeast Asia (Philippines, Laos) would require a slight increase in N_r inputs, as increased BNF, manure application, and atmospheric deposition would outweigh the decrease in mineral fertilizer application in these regions (Extended Data Fig. 4).

Manure recycling to croplands is expected to increase with the evolution of new farming methods and better integration of livestock and crop systems in the future[37]. To capture this, we added two supplementary scenarios as variants of the eCO_2 SSP2-4.5 scenario, improving the global manure N_r recycling ratio to 35% (manure recycle scenario 1) and 40% (manure recycle scenario 2) by 2050, respectively, relative to 30% in the base year 2020. This increased manure recycling to croplands would further decrease the need for synthetic fertilizer application overall. By 2050, N_r input from manure increases to 55 Tg N (from 51 Tg N), while fertilizer application declines from 141 Tg N to 98 Tg N under manure recycle scenario 1. Manure input increases to 75 Tg N, while fertilizer declines to 79 Tg N under manure recycle scenario 2 (Extended Data Fig. 5).

N_r emissions are projected to decrease globally, suggesting net positive effects on environmental and human health[38]. Our results show substantial reductions of N losses in East and South Asia, central eastern North America, south and eastern Latin America, followed by west and central Europe, sub-Saharan Africa, Southeast Asia and coastal South Australia under the eCO_2 SSP2-4.5 scenario (Fig. 2). N_r losses to the environment are modelled to be reduced through emissions of NH_3 (-12 Tg N), N_2O (-2 Tg N), NO_x (-0.9 Tg N), and leaching and runoff of NO_3^- to water bodies (-32 Tg N), while non-reactive N_2 emissions would increase by 7 Tg N due to enhanced denitrification processes in croplands (Fig. 3). The decrease of atmospheric NH_3 emissions mainly occurs in India and East China, the Great Lakes region in the United States, and East Argentina (Extended Data Fig. 6). N_2O emissions, in contrast, would increase in Central America, South and East Africa, South and East Asia, while decreasing in South Latin America and other regions. This regional difference can be attributed to interactions between increased emission factors of N_2O and reduced total N_r input to croplands under eCO_2. NO_x emissions are projected to slightly decline at global scale. NO_3^--N leaching and runoff to ground and surface water bodies is estimated to significantly decline, in particular in the river basins of India, China, Southeast Asia, Canada, and the United States.

Multiple scenario analysis and impact assessment

The ensemble average and the variations of N budgets in croplands under different future scenarios over 2020-2050 were estimated using Monte Carlo simulations with the CHANS model (Fig. 4). The time series of all baseline scenarios show consistently increasing N budgets in the near to mid-term, attributable to the continuous growth in food demand by 2050[2]. For instance, N_r harvested will increase from 192±5 Tg N in 2020 to 253±20 Tg N in 2050 under the baseline SSP2 scenario. The baseline N budgets of SSP2, representing a "business-as-usual" scenario, is higher than that of SSP1 representative of the "sustainable society" scenario, but similar to that of the SSP4 scenario, illustrating a "stratified society" scenario. All future eCO_2 scenarios show consistent N cycling responses to elevated atmospheric CO_2, with the more sustainability-focused scenarios resulting in lower budgets and their changes due to eCO_2. Mineral fertilizer application decline from baseline SSP1 scenario (115±10 to 128±30 Tg N) to eCO_2 SSP1-1.9 scenario (87±8 to 97±25 Tg N), while fertilizer application decreases from SSP4 scenario (129±11 to 142±32 Tg N) to eCO_2 SSP4-6.0 scenario (99±9 to 108±28 Tg N) over 2030-2050 (Fig. 4). The NO_3^- loss to water bodies will also reduce under eCO_2 scenarios, with smaller reductions in eCO_2 SSP1-1.9 scenario (26-30 Tg N) relative to that in eCO_2 SSP4-6.0 scenario (29-33 Tg N) over 2030-2050.

The impact assessment of eCO_2 as a single climate change driver on the global croplands in the absence of other concurrent climate change resulted in 672 billion US dollars benefit under eCO_2 SSP2-4.5 scenario in 2050, in terms of ecosystem benefit, human health benefit, yield increase, fertilizer saving, and climate impact (Fig. 5). China, India, North America, and Europe can gain the highest benefit, with the majority from ecosystem benefit and the sum accounting for 65% of the total benefits. The SSA (Sub-Saharan Africa) will get 20.6 billion US dollars from yield benefit. And the yield benefit is also significant for Brazil, China, India, and other Asian countries. The majority of eCO_2 impacts will lead to positive benefits, except that climate impact will cost 4.0, 4.4, and 0.3 billion US dollars in China, India and other OECD (organization for economic cooperation and development) countries. Ecosystem benefit accounts for the largest proportions of the total benefit (359 billion US dollars), followed by human health benefit (128 billion US dollars) and yield benefit (124 billion US dollars) globally. Therefore, elevated CO_2 as a single climate change factor can bring more benefit rather than damage to the ecosystem and humans. There is a caveat that other climate impacts are not accounted for in the monetized assessment, including changes in air temperature and precipitation, and extreme weather[4]. These consequences will damage the ecosystem and human health in the long term[13,15], leading to extra damage costs[39], which are not counted and also beyond the scope of this paper. We only focus on the direct costs and benefits of eCO_2 on the cropland N cycle and their impacts on the food benefit, environment and human health in this study.

Future perspective

While global ambitions to achieve NetZero+ are under way, these are unlikely to be achieved by 2050. Atmospheric CO_2 levels are likely to continue to increase for the foreseeable future[4]. This indicates that the changes in N cycles in global croplands as a response to eCO_2 are equally likely to become reality. Scientists, policymakers, farmers and other stakeholders will need to work together to adapt to these changes and design new approaches for agriculture management practices under elevated CO_2 levels[40]. We have to recognize and respond to these changes, especially increases in BNF, while the reduction of N_r inputs to croplands needs to be managed to avoid excessive N_r use[41]. In the context of the overall reduction of N_r input needs under eCO_2, the integrated management of N_r inputs between individual components becomes vitally important. The expected N Cycle changes provide a unique opportunity to reduce N_r inputs from mineral fertilizers, while increasing the reuse of manure and other organic N_r forms, such as straw recycling[42,43]. New crop varieties which are better adapted to higher CO_2 levels could be developed to further increase NUE and reduce N_r losses to the environment[44,45]. However, the decline of N_r concentrations in grain may adversely affect the supply of protein in human diets[18]. Thus, considerations of changes in future dietary recommendations may need to be adjusted to balance human nutritional requirements with grain protein supply[46].

However, the complexities associated with global warming and altered precipitation regimes, which will likely accompany elevated atmospheric CO_2 levels, and related impacts, will require integrated assessment approaches based on state-of-the-art complexity science methods in order to fully analyze and ultimately understand the response mechanisms of the N cycle to future climate change. This will be an essential step towards designing effective and efficient climate policy[47–49]. Adaptation of farming systems to higher crop yields and improved NUE will need to go hand in hand with measures to manage extreme climate impacts in order to reduce the uncertainties in future global crop production[16]. Our analyses suggest that we have the potential to supply more food to alleviate hunger and safeguard food security with less pollution under climate change conditions. However, the final impact of the complex interactions between the C and N cycles is not yet fully quantifiable and this potential is not robust. Whether the potential benefits to crop production and cropland NUE due to elevated CO_2 levels could offset some of the negative impacts of other climate change requires more attention and in-depth analyses. Our results highlight the importance of fully quantifying trade-offs and co-benefits between climate change factors which researchers and policy-makers alike must navigate in meeting climate change mitigation and sustainable development goals. A comprehensive and robust understanding of the response mechanisms of the N cycle to climate change will be a key requirement to constrain Earth System Models and inform the agricultural management and policy development in order to design future agricultural systems in the context of climate change[50]. Such robust, climate-resilient agricultural systems with reduced impacts on human and environmental health, while safeguarding food security, are vital for feeding a growing world population in a changing climate[51].

Materials and Methods

Database and global synthesis

A global database of elevated CO_2 simulation experiments was established through data extraction from site-based eCO_2 manipulation studies and data compilation from other data sources (Table S1). Elevated CO_2 manipulation studies mainly include FACE (free-air CO_2

enrichment), OTC (open-top chamber), and GC (growth chamber) experiments across the globe. The selection criteria of qualified studies mainly comprises: 1) elevated atmospheric CO_2 level was simulated in the manipulation experiments with eCO_2 group and control group (ambient CO_2); 2) variables related to N cycle or C cycle were monitored on a regular basis in both eCO_2 group and control group, and the values of the variables could be extracted from the study; 3) the studies were published in peer-reviewed journals included in authoritative databases such as Web of Science, Google Scholar, Scopus, and so on. A Cross search of publications was conducted in the meantime. The systematic literature search contained but was not limited to the following key terms: {(elevated CO2/ rising CO2/ CO2 fertilization) OR (FACE/ OTC/ GC)} AND {(nitrogen fixation/ BNF/ nitrogen use efficiency/ NUE/ denitrification/ NH3/ ammonia/ N2O/ nitrous oxide/ nitrogen leaching/ nitrogen runoff/ nitrogen mineralization/ nitrification/ nitrogen cycle) OR (yield/ SOC/ soil organic carbon/ soil respiration/ Rs/ nitrogen content/ C:N ratio/ carbon cycle)}. We collected the main four categories of information from the studies, including paper information (author, year, title, journal, etc.), site information (latitude, longitude, climate, soil texture, country, etc.), study information (experimental duration, manipulation method, manipulation magnitude, etc.), and variable information (response ratio, sample size, etc.). The terminology used in the study can be found in the Supplementary Text.

Data of variables were extracted from the text, tables, and figures in the published papers. WebPlotDigitizer was used to extract data from figures (https://apps.automeris.io/wpd/). Meanwhile, data from other sources were compiled into our database to supplement the missing information in some publications, i.e., climate data, soil texture, climate zones. Climate data of study sites (i.e., mean annual temperature, mean annual precipitation, maximum temperature, and minimum temperature) was obtained from the WorldClim (https://worldclim.org/data/index.html#). Soil texture was from the Global Land Data Assimilation System (GLDAS) by NASA (https://ldas.gsfc.nasa.gov/gldas/soils). Assignment of climate zone was based on Köppen-Geiger climate classification[52].

Meta-analysis was conducted to assess the response ratio (*RR*) of N and C cycling variables under eCO_2 relative to ambient CO_2 level. The response ratio of individual observation in natural logarithm (*lnR*) was calculated as[53]:

$$lnR = \ln \frac{x_{eCO2}}{x_{aCO2}} \qquad \text{(Equation 1)}$$

Where x_{eCO2} and x_{aCO2} are the means of parameters at elevated CO_2 level and ambient CO_2 level, respectively.

The weight of individual observations was calculated based on the experimental replications as[54]:

$$Weight = \frac{n_{eCO2} \times n_{aCO2}}{n_{eCO2} + n_{aCO2}} \qquad \text{(Equation 2)}$$

where n_{eCO2} and n_{aCO2} are numbers of the replications at elevated CO_2 level and ambient CO_2 level, respectively.

The mean response ratio (*RR*) and 95% confidence intervals were generated following a randomization resampling procedure by bootstrapping (4,999 iterations). The results were reported as percentage changes for easy demonstration:

$$RR\% = (e^{RR}-1)\times 100\% \quad \text{(Equation 3)}$$

The response ratio was considered significant (P<0.05) if the 95% confidence intervals did not overlap with zero.

Subgroup analysis and meta-regression were adopted to explore the moderators and spatial heterogeneity of response patterns. The *RR*s were divided into different subgroups by crop group (i.e., wheat, soybean, oilseeds, barley, cotton), manipulation methods (i.e., FACE, OTC, GC), or climate zones (i.e., cold, temperate, arid, tropical) for meta-analysis. The significant between-group heterogeneity (Q_b) (P<0.05) denotes significant difference among subgroups. Meta-regressions were used to test whether the potential moderators can affect the response pattern across locations, including manipulation magnitude (ΔCO_2), mean annual temperature (MAT), and mean annual precipitation (MAP).

The statistical analysis was done with the software *MetaWin*[55] and *metafor* package[56] in R platform (version 4.1.3).

Global cropland nitrogen budget

The accounting of cropland N budget is to identify N input (N_{input}), N harvest ($N_{harvest}$), N surplus ($N_{surplus}$), and NUE, on the foundation of the N mass balance principle. The calculation formulas are shown as follows:

$$\sum_1^i N_{input} = \sum_1^j N_{harvest} + \sum_1^k N_{surplus} \quad \text{(Equation 4)}$$

$$NUE_i = \frac{N_{harvest,i}}{N_{input,i}} \quad \text{(Equation 5)}$$

$$N_{input,i} = N_{fer,i} + N_{BNF,i} + N_{man,i} + N_{dep,i} + N_{other,i} \quad \text{(Equation 6)}$$

$$N_{surplus,i} = N_{gas,i} + N_{water,i} \quad \text{(Equation 7)}$$

where N_{input} contains five components, i.e., synthetic fertilizer ($N_{fer,i}$), BNF ($N_{BNF,i}$), manure ($N_{man,i}$), deposition ($N_{dep,i}$), and other inputs ($N_{other,i}$); $N_{harvest}$ refers to harvested crops consisting of grain and straw; $N_{surplus}$ contains three components, i.e., gaseous N loss (NH_3, N_2O, NO_x, N_2) ($N_{gas,i}$) and N loss to water (leaching to groundwater & runoff to surface water, NO_3^-) ($N_{water,i}$).

The input factor ($F_{input,i}$) and emission factor ($F_{emit,i}$) is defined as:

$$F_{input,i} = \frac{N_{input\cdot component,i}}{N_{input,i}} \quad \text{(Equation 8)}$$

$$F_{emit,i} = \frac{N_{emit\cdot component,i}}{N_{surplus,i}} \quad \text{(Equation 9)}$$

where $N_{input\ component,i}$ could be any component of N_{input}, that is, $N_{fer,i}$, $N_{BNF,i}$, $N_{man,i}$, $N_{dep,i}$; $N_{emit\ component,i}$ could be any component of $N_{surplus,i}$, such as $N_{gas,i}$ and $N_{water,i}$.

The reactive N ($N_{r,i}$) flows include NH_3 flows ($N_{NH3,i}$), N_2O flows ($N_{N2O,i}$), NO_x flows ($N_{NOx,i}$), and N loss to water ($N_{water,i}$):

$$N_{r,i} = N_{NH_3,i} + N_{N_2O,i} + N_{NO_x,i} + N_{water,i} \quad \text{(Equation 10)}$$

The present and future global cropland N budgets at 0.5 by 0.5 degree resolution are generated based on the Integrated Model to Assess the Global Environment (IMAGE)[36,57] and the Coupled Human And Natural System (CHANS)[22] models. IMAGE is an ecological-environmental model simulating environmental consequences of human activities via integrating society, biosphere, and climate system in one framework (https://www.pbl.nl/en/image/about-image). CHANS is a process-based model that simulates N-flow within 14 subsystems (i.e., cropland, grassland, forest, atmosphere, surface water and groundwater)[22]. Here gridded data of global cropland budget (0.5 by 0.5 degree) in the base year 2020 was exported from the IMAGE model, and then input to the CHANS model for validation and optimization with the historical data at the country-level embedded in the CHANS model, for minimizing the uncertainties of global cropland N budget (Fig. S1). Future crop harvests from 2030 to 2050 at 10-yr intervals are constrained by the future prediction data from Food and Agriculture Organization (FAO) Global perspective study[58], which mainly projects future crop yield and harvest area based on food demand depending on population, gross domestic production, and urbanization rates.

Scenario and CHANS model simulation

Aiming to estimate the changes of N budget under future elevated CO_2 levels, we designed the baseline scenario (no climate change) and eCO_2 scenario, respectively, each containing three sub-scenarios with different Shared Socio-economic Pathways (SSPs) (Extended Data Fig. 3). The baseline scenario hypotheses no climate change will occur in the future and the atmospheric CO_2 levels will not continue to rise and will stay at a fixed level since 2020. The eCO_2 scenario hypotheses only elevated atmospheric CO_2 as a single factor of climate change will be anticipated and eCO_2 be taken into account in our modelling simulating of future trend, without consideration of associated warming and changing precipitation; future atmospheric CO_2 levels were applied from Representative Concentration Pathways (RCPs) including RCP1.9, RCP4.5, and RCP6.0. As the climate change factor was set in the baseline and eCO_2 scenarios, SSPs provide storylines and narratives about the social-economic aspect for future projection. SSP1, SSP2, and SSP4 were adopted in our study, corresponding to Sustainable society, Business as usual, and Stratified society in the Global Perspective studies by FAO[58]. Thus, the baseline scenario with no climate change has three sub-scenarios including SSP1, SSP2, and SSP4, meaning different socio-economic pathways have been considered in modelling to influence the population and GDPs, leading to changes in harvest crops demand and supply, fertilizer use demand, and NUEs. Accordingly, the eCO_2 scenarios have sub-scenarios of SSP1-RCP1.9, SSP2-4.5, and SSP4-RCP6.0, considering both social-economic pathways and eCO_2 as a single indicator of climate change for modelling.

We conducted CHANS model simulation for N budgeting based on the above scenarios. The base year is 2020 and the future trend from 2030 to 2050 will be projected. In the baseline scenarios, mainly the social-economic indexes of population, GDP, and urbanization are considered to project future food production; but no climate change effects are considered in modelling given the fixed CO_2 level since 2020. The model outputs of future cropland N budgets were validated and constrained by the FAO future prediction in 2030-2050[58]. In the

eCO_2 scenarios, in addition to the social-economic indexes, we simulate rising CO_2 levels by integrating the response ratios of N cycling parameters to the CHANS model and optimizing parameterization with results of our global synthesis of site-based observations. The historical atmospheric CO_2 levels were reconstructed from CMIP6 historical data and future atmospheric CO_2 levels were generated under SSP-RCPs[31].

The effects of eCO_2 on crop yield and grain content for various crop items were incorporated into the crop production dataset of future prediction in 2030-2050 from FAO[58]. The crop production by country is summed up as follows:

$$N_{\text{harvest}}^{base} = \sum_1^i \left(Yield_{crop,i} \times GrainN_{crop,i} \times Area_{crop,i}\right) \quad \text{(Equation 11)}$$

$$N_{\text{harvest}}^{eCO_2} = \sum_1^i \left(Yield_{crop,i} \times \left(1 + RR\%_{yield}\right) \times GrainN_{crop,i} \times \left(1 + RR\%_{GrainN}\right) \times Area_{crop,i}\right) \quad \text{(Equation 12)}$$

where $N_{harvest}^{base}$ and $N_{harvest}^{eCO2}$ indicate N harvests in the country under the baseline scenario and the eCO_2 scenario, respectively; $Yield_{crop,i}$ is the yield of the specific crop item, and the *crop i* indicates the specific crop item; $GrainN_{crop,i}$ is the N content in the grain; $Area_{crop,i}$ refers to the harvest area of the crop item; $RR\%_{yield}$ and $RR\%_{GrainN}$ denote the response ratios of yield and grain N content to eCO_2, respectively. The responses of yield and grain N content are moderated with the regional ΔCO_2, MAT and MAP, and constrained by maximum yield potential, and the upper and lower limit of 95% confidential intervals from the meta-analysis.

The effects of eCO_2 on N cycling parameters (NUE_i, $N_{BNF,i}$, $N_{fer,i}$, $N_{NH3,i}$, $N_{water,i}$, etc.) were scaled up to modify the NUE, input factor ($F_{input,i}$) or emission factor ($F_{emit,i}$) in the CHANS model. The NUE under the elevated CO_2 is calculated as NUE_i^{eCO2} as:

$$NUE_{\text{i}}^{eCO_2} = NUE_i \times \left(1 + RR\%_{NUE,i}\right) \quad \text{(Equation 13)}$$

where $RR\%_{NUE}$ denote the response ratios in percentage change for NUE.

The factors coupled with eCO_2 effects are calculated as $F_{input,i}^{eCO2}$ and $F_{emit,i}^{eCO2}$ as:

$$F_{input,i}^{eCO_2} = \frac{N_{input\cdot component,i}}{N_{input,i}} \times \left(1 + RR\%_{input\cdot component,i}\right) \quad \text{(Equation 14)}$$

$$F_{emit,i}^{eCO_2} = \frac{N_{emit\cdot component,i}}{N_{surplus,i}} \times \left(1 + RR\%_{emit\cdot component,i}\right) \quad \text{(Equation 15)}$$

where $RR\%_{input\ component}$ and $RR\%_{emit\ component}$ denote the response ratios in percentage change for N input factor and emission factor, respectively.

CHANS model simulation to predict future cropland N budget is performed with the gridded dataset of global cropland N budget, depending on the regional patterns and geographical heterogeneity. Responses of NUE modulated by the local MAP within the confidential intervals in the meta-analysis are allocated as $RR\%_{NUE,i}$ to the gridded data (Extended Data Fig. 2). Responses of BNF in different climate zones are allocated to the gridded data (Fig. S4). Changes in response factors of deposition depend on the summed NH_3 and NO_x emissions. Responses factors of NH_3 and N_2O are moderated with ΔCO_2 and then incorporated into the model. As the NO_x emission from the cropland is minimum and the metadata of NO_x in cropland is lacking, we use response ratios of NO_x in the terrestrial ecosystem for substitution. Responses of NO_3^- are allocated as $RR\%_{water,i}$.

Here anthropogenic N input acts as a flexible component of input, with the assumption that the use of fertilizer will adapt to the changing soil fertility. The scenario period over 2020-2050 is middle to long term, farmers will adjust the amount of fertilizer with the evolvement of soil nutrient condition depending on altered NUE and natural N input (i.e., BNF, deposition). In the basic eCO_2 scenarios above, the changes are mainly allocated to the input factors of synthetic fertilizer ($N_{fer,i}$) and the input factors of manure stay constant. However, future use of organic fertilizer –manure ($N_{man,i}$)– will probably increase with the development of agriculture. Thereby we design two supplementary scenarios based on eCO_2 SSP2-4.5 scenario (with the same climate change setting) (Extended Data Fig. 3). We improve the global mean of manure recycling ratio to 35% (manure recycle scenario 1) and 40% (manure recycle scenario 2) by 2050 relative to the manure recycling ratio of 30% in base year 2020, aiming to assess the possible changes in synthetic fertilizer under higher manure recycling in the future.

Impact assessment

The potential impacts of elevated CO_2 (M_{eCO2}) as a single climate change factor in global cropland constitutes of ecosystem impact (B_{eco}), human health impact (B_{human}), yield change (B_{yield}), fertilizer saving (B_{fer}), and climate impact ($M_{climate}$) as the following equation:

$$I_{eCO_2} = \sum_1^i \left(I_{eco} + I_{human} + I_{yield} + I_{fer} + I_{climate} \right) \quad \text{(Equation 16)}$$

The comprehensive monetary impact analysis of elevated CO_2 is conducted at the national scale and then scaled up to regional and global cropland by categorizing country groups.

The ecosystem impact is defined as the changed damage cost of Nr effects on the ecosystem service. The ecosystem impact for country/ region *i* ($B_{eco,i}$) can be calculated as:

$$I_{eco,i} = \Delta N_{r,i} \times d_{eco,EU} \times \frac{WTP_i}{WTP_{EU}} \times \frac{PPP_i}{PPP_{EU}} \quad \text{(Equation 17)}$$

where $\Delta N_{r,i}$ is the changes of Nr including NH_3 flows, N_2O flows, NO_x flows, and N loss to water for country or area *i*; $d_{eco,EU}$ stands for the estimated ecosystem damage cost of Nr emission in the European Union (EU) based on the European N Assessment[59]; WTP_i and WTP_{EU} denote the values of the willingness to pay for ecosystem service in the country/ area *i* and the EU, respectively; $PPP_{i,j}$ and $PPP_{EU,j}$ denote the purchasing power parity of the country/ area *i* and the EU. Here we apply the ecosystem damage cost of Nr emission in EU to other countries after corrections using willingness to pay and purchasing power parity, aiming to attain the comparable ecosystem benefit across the globe[60]. Several cost and benefit studies concerning the effects of Nr on the ecosystem have been conducted in Europe and the United States, and there is a paucity of available data in other areas or countries[60,61].

The human health impact is defined as the changed health damage due to varied Nr emissions under elevated CO_2 levels. The monetary estimate of human health is as follows:

$$I_{human,i} = \Delta N_{r,i} \times d_{human,i} \quad \text{(Equation 18)}$$

where $\Delta N_{r,i}$ is the changes of Nr for country or area i; $d_{human,i}$ stands for the human health damage cost of Nr emission for country/area i, which is calculated based on the metric of N-share to $PM_{2.5}$ pollution[12], i.e. the contribution of Nr compounds to the total $PM_{2.5}$ concentration determined by modeling with and without Nr emission.

The monetary evaluation of yield change can be calculated as the changed crop revenues from crop harvest using the following equation:

$$I_{yield,i} = \Delta N_{harvest,i}^{eCO_2} \times p_{yield,i} \quad \text{(Equation 19)}$$

where $\Delta N_{harvest,i}^{eCO2}$ is the changes in N harvest under elevated CO_2 scenario relative to baseline scenario for country or area i; $p_{yield,i}$ is the crop price in the specific country or area i, in US dollars per kg N.

The fertilizer saving refers to the saved investment of N fertilizer to croplands due to reductions in synthetic fertilizer input under elevated CO_2 scenarios as:

$$I_{fer,i} = \Delta N_{fer,i} \times p_{fer} \quad \text{(Equation 20)}$$

where $\Delta N_{fer,i}$ is the changes in N fertilizer input under elevated CO_2 scenario relative to baseline scenario for country or area i; p_{fer} is the N fertilizer price, in US dollars per kg N.

The climate impact can be positive or negative for different countries and regions, resulting in either benefit or damage costs in certain countries and regions. The potent greenhouse gas N_2O makes a contribution to global warming implying a negative climate impact. Whereas, NO_x and NH_3 are vital precursors of aerosols, which would reflect long-wave solar radiation and have a strong cooling impact on the climate system[62]. Thereby the cost-benefit analysis of climate impact is conducted as follows:

$$I_{climate} = \Delta N_{r,i} \times m_{climate,i} \quad \text{(Equation 21)}$$

where $\Delta N_{r,i}$ is the changes of Nr for country or area i; $m_{climate,i}$ stands for the unit climate damage or benefit of Nr emission for country/area i, in US dollars per kg N.

Uncertainty analysis

Uncertainty analysis of the cropland N budget was conducted by running the Monte Carlo simulations with the CHANS model by 1,000 iterations. Monte Carlo simulation is a statistical test method to simulate the real situation by random resampling. In the CHANS model of the N budget, the uncertainty sources and uncertainty ranges of input parameters are identified according to the data distribution and characteristics. Basically, the coefficients of variation (CV) were used to represent the relative uncertainty ranges of cropland N budget data, and the standard deviations (SD) were used to represent the relative uncertainty ranges of climate change impact under elevated CO_2 (Table S2). After 1,000 iterations of CHANS model simulations, the average and the variations of N budgets can be calculated from projection ensembles.

Acknowledgments

This study was supported by the National Natural Science Foundation of China (42261144001, 42061124001 and 41822701), National Key Research and Development Project of China (2022YFD1700014, 2022YFD1700700), and Pioneer and Leading Goose R&D Program of Zhejiang (2022C02008). We thank Miao Zheng and Ziyue Qiu for their hard work on meta-data collection and validation.

Author contributions

B.G. and J.C. designed the study. J.C. performed the research and analyzed the data. B.G. and J.C. interpreted the results and wrote the first draft of the paper. X.Z. provided data and analysis support. S.R. reviewed and edited the paper. C.W. and H.C. collected data from climate change experiments. S.W. and P.H. provided visualization support. H.G. provided modelling support. All authors contributed to the discussion and revision of the paper.

Competing interests

The authors declare no competing interests.

Data availability

Data on the main findings can be found in Supplementary Information. Further data that support the findings of this study are collected from online open databases or literature sources as cited.

References

1. Galloway, J. N. *et al.* Transformation of the nitrogen cycle: Recent trends, questions, and potential solutions. *Science.* **320**, 889–892 (2008).
2. Tilman, D., Balzer, C., Hill, J. & Befort, B. L. Global food demand and the sustainable intensification of agriculture. *Proc. Natl. Acad. Sci. U. S. A.* **108**, 20260–20264 (2011).
3. Wheeler, T. & Von Braun, J. Climate change impacts on global food security. *Science.* **341**, 508–513 (2013).
4. IPCC. Summary for Policymakers. in *Climate Change 2021: The Physical Science Basis* (Cambridge university press, 2021).
5. Xia, L. *et al.* Elevated CO_2 negates O_3 impacts on terrestrial carbon and nitrogen cycles. *One Earth* **4**, 1752–1763 (2021).
6. Ainsworth, E. A. & Long, S. P. 30 years of free-air carbon dioxide enrichment (FACE): What have we learned about future crop productivity and its potential for adaptation? *Glob. Chang. Biol.* **27**, 27–49 (2021).
7. Zaehle, S., Jones, C. D., Houlton, B., Lamarque, J. F. & Robertson, E. Nitrogen availability reduces CMIP5 projections of twenty-first-century land carbon uptake. *J. Clim.* **28**, 2494–2511 (2015).
8. Yue, K. *et al.* Influence of multiple global change drivers on terrestrial carbon storage: additive effects are common. *Ecol. Lett.* **20**, 663–672 (2017).
9. Van Groenigen, K. J., Qi, X., Osenberg, C. W., Luo, Y. & Hungate, B. A. Faster decomposition under increased atmospheric CO_2 limits soil carbon storage. *Science.* **344**, 508–509 (2014).

10. Gruber, N. & Galloway, J. N. An Earth-system perspective of the global nitrogen cycle. *Nature* **451**, 293–296 (2008).
11. Sutton, M. A. *et al.* Too much of a good thing. *Nature* **472**, 159–161 (2011).
12. Gu, B. *et al.* Abating ammonia is more cost-effective than nitrogen oxides for mitigating $PM_{2.5}$ air pollution. *Science.* **374**, 758–762 (2021).
13. Sinha, E., Michalak, A. M. & Balaji, V. Eutrophication will increase during the 21st century as a result of precipitation changes. *Science.* **357**, 1–5 (2017).
14. Rosenzweig, C. *et al.* Assessing agricultural risks of climate change in the 21st century in a global gridded crop model intercomparison. *Proc. Natl. Acad. Sci. U. S. A.* **111**, 3268–3273 (2014).
15. Zhu, P. *et al.* Warming reduces global agricultural production by decreasing cropping frequency and yields. *Nat. Clim. Chang.* (2022).
16. Lobell, D. B., Schlenker, W. & Costa-Roberts, J. Climate trends and global crop production since 1980. *Science.* **333**, 616–620 (2011).
17. Mason, R. E. *et al.* Evidence, causes, and consequences of declining nitrogen availability in terrestrial ecosystems. *Science.* **376**, (2022).
18. Beach, R. H. *et al.* Combining the effects of increased atmospheric carbon dioxide on protein, iron, and zinc availability and projected climate change on global diets: a modelling study. *Lancet Planet. Heal.* **3**, e307–e317 (2019).
19. Wuepper, D., Le Clech, S., Zilberman, D., Mueller, N. & Finger, R. Countries influence the trade-off between crop yields and nitrogen pollution. *Nat. Food* **1**, 713–719 (2020).
20. Stevens, C. J. Nitrogen in the environment. *Science.* **363**, 578–580 (2019).
21. Bouskill, N. J., Riley, W. J. & Tang, J. Y. Meta-analysis of high-latitude nitrogen-addition and warming studies implies ecological mechanisms overlooked by land models. *Biogeosciences* **11**, 6969–6983 (2014).
22. Gu, B., Ju, X., Chang, J., Ge, Y. & Vitousek, P. M. Integrated reactive nitrogen budgets and future trends in China. *Proc. Natl. Acad. Sci. U. S. A.* **112**, 8792–8797 (2015).
23. Gu, B. *et al.* Toward a Generic Analytical Framework for Sustainable Nitrogen Management: Application for China. *Environ. Sci. Technol.* **53**, 1109–1118 (2019).
24. Wang, B. *et al.* Air warming and CO_2 enrichment increase N use efficiency and decrease N surplus in a Chinese double rice cropping system. *Sci. Total Environ.* **706**, (2020).
25. Lam, S. K. *et al.* Effect of elevated carbon dioxide on growth and nitrogen fixation of two soybean cultivars in northern China. *Biol. Fertil. Soils* **48**, 603–606 (2012).
26. Moser, G. *et al.* Explaining the doubling of N_2O emissions under elevated CO_2 in the Giessen FACE via in-field ^{15}N tracing. *Glob. Chang. Biol.* **24**, 3897–3910 (2018).
27. Taub, D. R. & Wang, X. Why are nitrogen concentrations in plant tissues lower under elevated CO_2? A critical examination of the hypotheses. *J. Integr. Plant Biol.* **50**, 1365–1374 (2008).
28. Wang, W. *et al.* Yield, dry matter distribution and photosynthetic characteristics of rice under elevated CO_2 and increased temperature conditions. *F. Crop. Res.* **248**, 107605 (2020).
29. Sardans, J. *et al.* Changes in nutrient concentrations of leaves and roots in response to

global change factors. *Glob. Chang. Biol.* **23**, 3849–3856 (2017).
30. Guo, Y. *et al.* Enhanced leaf turnover and nitrogen recycling sustain CO_2 fertilization effect on tree-ring growth. *Nat. Ecol. Evol.* **6**, 1271–1278 (2022).
31. Cheng, W. *et al.* Global monthly gridded atmospheric carbon dioxide concentrations under the historical and future scenarios. *Sci. Data* **9**, 1–13 (2022).
32. FAO, IFAD, UNICEF, WFP & WHO. *The State of Food Security and Nutrition in the World 2021. The State of Food Security and Nutrition in the World 2021* (2021).
33. Zhang, X. *et al.* Managing nitrogen for sustainable development. *Nature* **528**, 51–59 (2015).
34. Liu, L. *et al.* Exploring global changes in agricultural ammonia emissions and their contribution to nitrogen deposition since 1980. *Proc. Natl. Acad. Sci. U. S. A.* **119**, 1–9 (2022).
35. Quemada, M. *et al.* Exploring nitrogen indicators of farm performance among farm types across several European case studies. *Agric. Syst.* **177**, 102689 (2020).
36. van Grinsven, H. J. M. *et al.* Establishing long-term nitrogen response of global cereals to assess sustainable fertilizer rates. *Nat. Food* **3**, 122–132 (2022).
37. Gu, B. Recoupling livestock and crops. *Nat. Food* **3**, 102–103 (2022).
38. Steffen, W. *et al.* Planetary boundaries: Guiding human development on a changing planet. *Science.* **347**, 1259855 (2015).
39. Rennert, K. *et al.* Comprehensive Evidence Implies a Higher Social Cost of CO_2. *Nature* **610**, (2022).
40. Dobermann, A. *et al.* Responsible plant nutrition: A new paradigm to support food system transformation. *Glob. Food Sec.* **33**, 100636 (2022).
41. Gu, B. *et al.* A Credit System to Solve Agricultural Nitrogen Pollution. *Innov.* **2**, 100079 (2021).
42. Shyamsundar, P. *et al.* Fields on fire: Alternatives to crop residue burning in India. *Science.* **365**, 536–538 (2019).
43. Bai, Z. *et al.* Relocate 10 billion livestock to reduce harmful nitrogen pollution exposure for 90% of China’s population. *Nat. Food* **3**, 152–160 (2022).
44. Korres, N. E. *et al.* Cultivars to face climate change effects on crops and weeds: a review. *Agron. Sustain. Dev.* **36**, 1–22 (2016).
45. Wei, S. *et al.* A transcriptional regulator that boosts grain yields and shortens the growth duration of rice. *Science.* **377**, (2022).
46. Springmann, M. *et al.* Global and regional health effects of future food production under climate change: A modelling study. *Lancet* **387**, 1937–1946 (2016).
47. Rillig, M. C. *et al.* The role of multiple global change factors in driving soil functions and microbial biodiversity. *Science.* **366**, 886–890 (2019).
48. Yue, K. *et al.* Responses of nitrogen concentrations and pools to multiple environmental change drivers: A meta-analysis across terrestrial ecosystems. *Glob. Ecol. Biogeogr.* **28**, 690–724 (2019).
49. Lesk, C., Coffel, E. & Horton, R. Net benefits to US soy and maize yields from intensifying hourly rainfall. *Nat. Clim. Chang.* **10**, (2020).
50. Chrysafi, A. *et al.* Quantifying Earth system interactions for sustainable food production via expert elicitation. *Nat. Sustain.* (2022).
51. Bowles, T. M. *et al.* Addressing agricultural nitrogen losses in a changing climate. *Nat.*

Sustain. **1**, 399–408 (2018).
52. Beck, H. E. *et al.* Present and future köppen-geiger climate classification maps at 1-km resolution. *Scientific Data* vol. 5 (2018).
53. Hedges, L. V., Gurevitch, J. & Curtis, P. S. The meta-analysis of response ratios in experimental ecology. *Ecology* **80**, 1150 (1999).
54. Pittelkow, C. M. *et al.* Productivity limits and potentials of the principles of conservation agriculture. *Nature* **517**, 365–368 (2015).
55. Rosenberg, M., Adams, D. & Gurevitch, J. MetaWin: Statistical software for meta-analysis. Version 2.0. *Sinauer Assoc.* (2000).
56. W, V. Conducting meta-analyses in R with the metafor package. *J. Stat. Softw.* **36**, 1–48 (2010).
57. Beusen, A. H. W. *et al.* Exploring river nitrogen and phosphorus loading and export to global coastal waters in the Shared Socio-economic pathways. *Global Environmental Change* vol. 72 (2022).
58. FAO. *The future of food and agricutlure - Alternative pathways to 2050. Summary version*. *Summary Version* (2018).
59. Kristal, S. L., Randall-Kristal, K. A. & Thompson, B. M. *The Society for Academic Emergency Medicine's 2004-2005 Emergency Medicine Faculty Salary and Benefit Survey*. *Academic Emergency Medicine* vol. 13 (2006).
60. Van Grinsven, H. J. M. *et al.* Costs and benefits of nitrogen for europe and implications for mitigation. *Environ. Sci. Technol.* **47**, 3571–3579 (2013).
61. Sobota, D. J., Compton, J. E., McCrackin, M. L. & Singh, S. Cost of reactive nitrogen release from human activities to the environment in the United States. *Environ. Res. Lett.* **10**, (2015).
62. Zhang, X. *et al.* Societal benefits of halving agricultural ammonia emissions in China far exceed the abatement costs. *Nat. Commun.* **11**, 1–10 (2020).

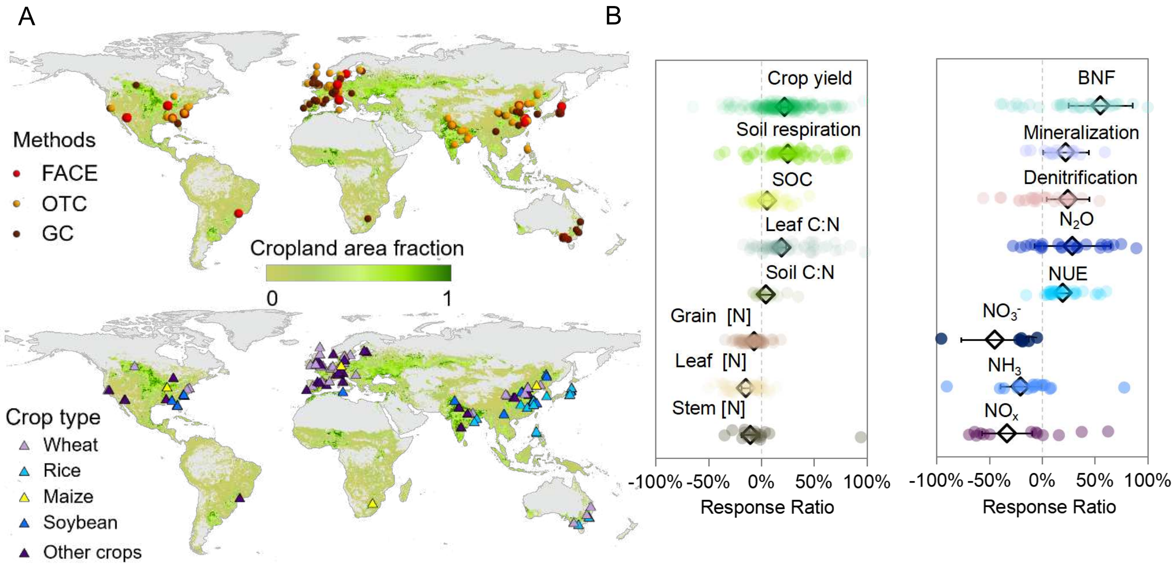

Fig. 1 Effects of elevated CO_2 levels (eCO_2) on nitrogen and carbon cycles in global croplands. (A) Maps displaying the distribution of experimental sites simulating elevated atmospheric CO_2 levels, by different manipulation methods (FACE, Free-Air CO_2 Enrichment; OTC, Open-Top Chamber; GC, Greenhouse & Growth Chamber), and by various crop types. The global cropland area fractions are shown as 0-1. **(B)** Relative effects of elevated CO_2 levels on main variables of nitrogen and carbon cycling versus ambient atmospheric CO_2 levels. Scatter plots in color represent response ratios of observations from the meta database, and the diamonds with error bars indicate mean values of response ratios with a 95% confidence interval based on the meta-analysis. The value of response ratio is significant if the 95% confidence interval does not overlap zero. SOC, soil organic carbon; Grain [N], grain N content; Leaf [N], leaf N content; Stem [N], stem N content; BNF, biological N fixation; NUE, N use efficiency.

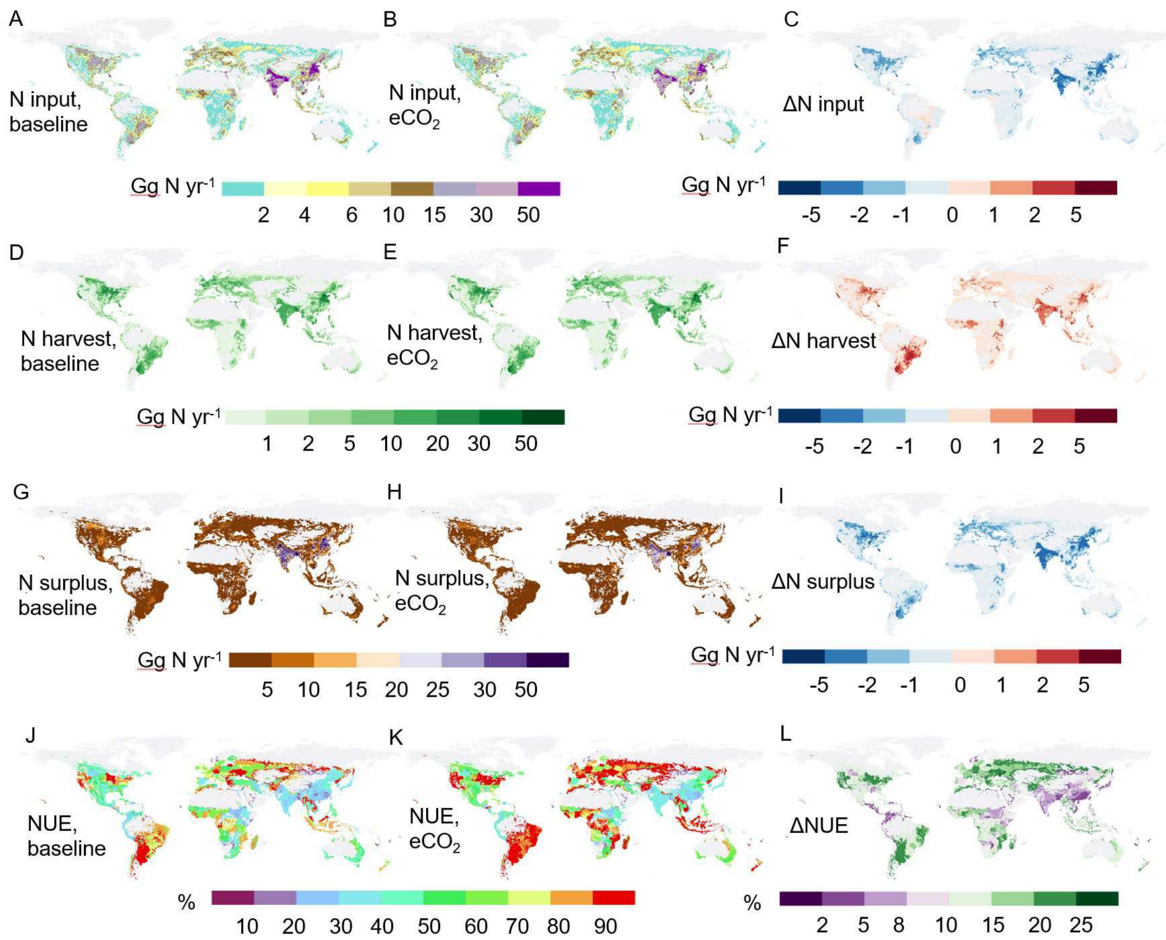

Fig. 2 N budgets of global cropland and their changes between baseline scenario (no climate change) and elevated CO_2 scenario (SSP2-4.5) in 2050. N input in baseline scenario (**A**), eCO_2 scenario (**B**), and ΔN input (**C**); N harvest in baseline scenario (**D**), eCO_2 scenario (**E**), and ΔN harvest (**F**); N surplus (N_r loss & N_2) in baseline scenario (**G**), eCO_2 scenario (**H**), and ΔN surplus (**I**); N use efficiency in baseline scenario (**J**), eCO_2 scenario (**K**), and ΔN harvest (**L**). Values in the legend reflect the average annual N budget from cropland within a grid cell (0.5 by 0.5 degree). Base map is applied without endorsement from Natural Earth (https://www.naturalearthdata.com/).

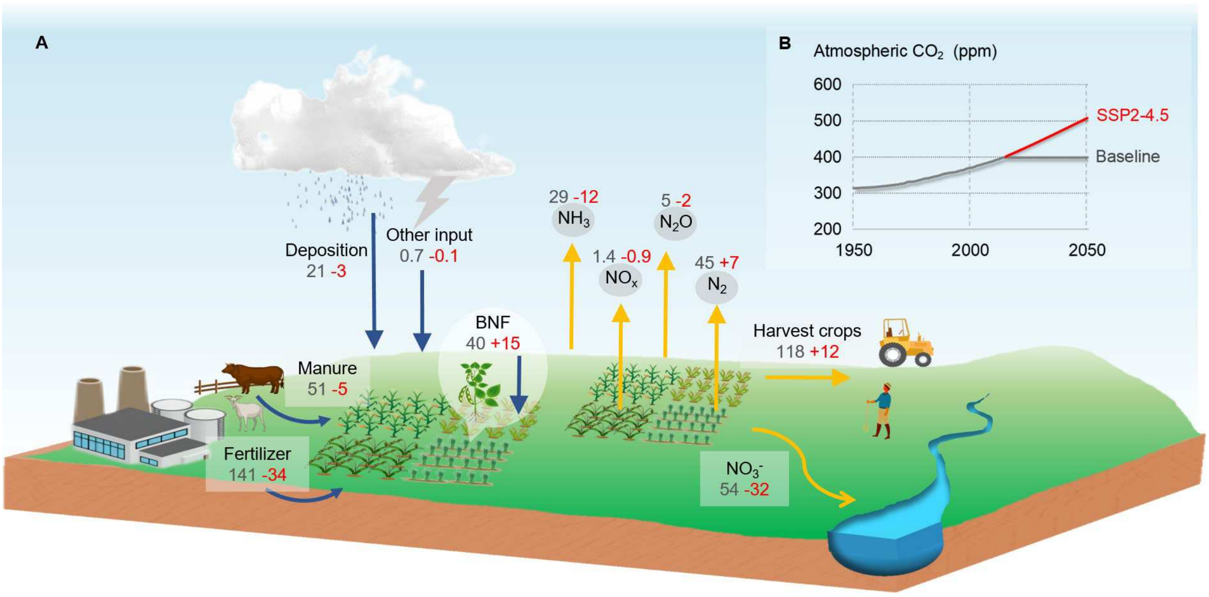

Fig. 3 N flows in global croplands under elevated CO_2 scenario (SSP2-4.5) by 2050. (**A**) N input and N output constitute the major N flows, represented by blue and yellow arrows, respectively. Values of N flows in dark grey denote flows in the baseline scenario with no climate change, while the red flows denote changes in flows under elevated CO_2 scenario (SSP2-4.5) relative to the baseline scenario. The numbers are future values derived from our simulations in Tg N per year by 2050. (**B**) Historical and future atmospheric CO_2 levels in the baseline scenario and elevated CO_2 scenario during 1950-2050.

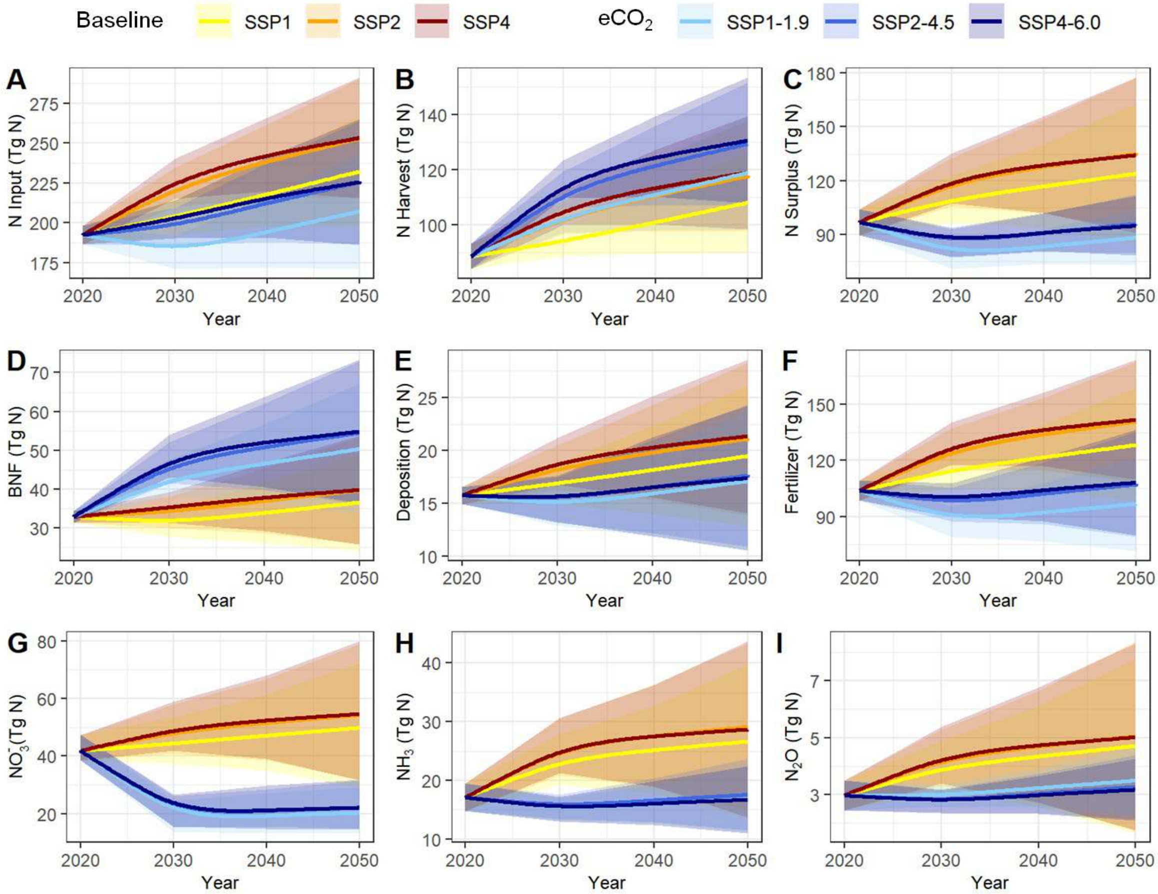

Fig. 4 Time series of N budget in global cropland over 2020-2050 under future scenarios. Solid lines represent total N input (**A**), N harvest (**B**), N surplus (N_r loss & N_2) (**C**), BNF (biological N fixation) (**D**), deposition (**E**), fertilizer (**F**), NO_3^- (**G**), NH_3 (**H**), N_2O (**I**), from global cropland per year under baseline scenarios and elevated CO_2 scenarios. Shading represents standard deviation.

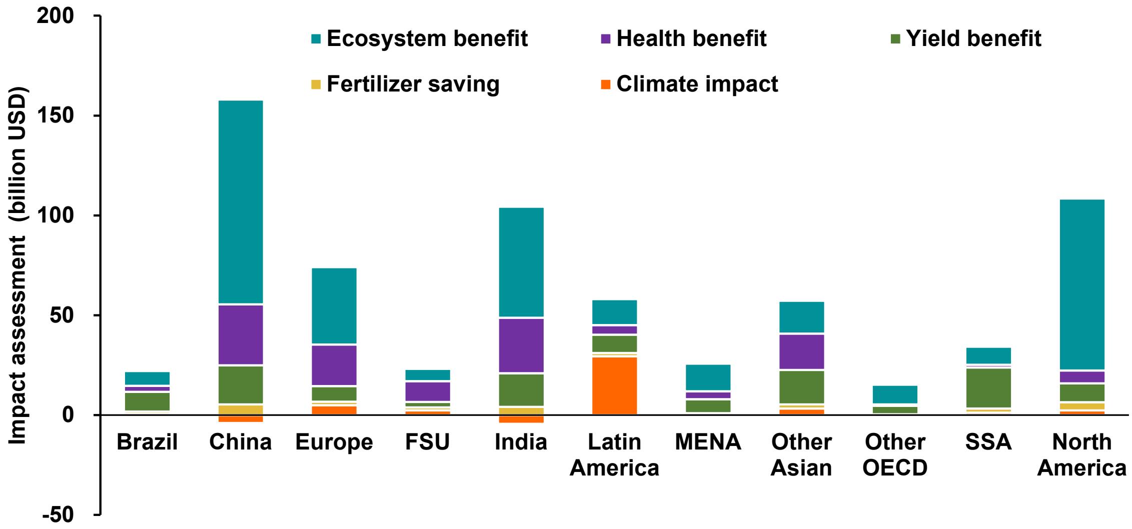

Fig. 5 Impact assessment of elevated atmospheric CO_2 levels as a single climate change factor under SSP2-4.5 scenario relative to baseline scenario with no climate change in 2050. The positive values indicate benefit and negative values indicate damage cost. FSU, Former Soviet Union; MENA, Middle East and North Africa; OECD, organization for economic cooperation and development; SSA, Sub-Saharan Africa.

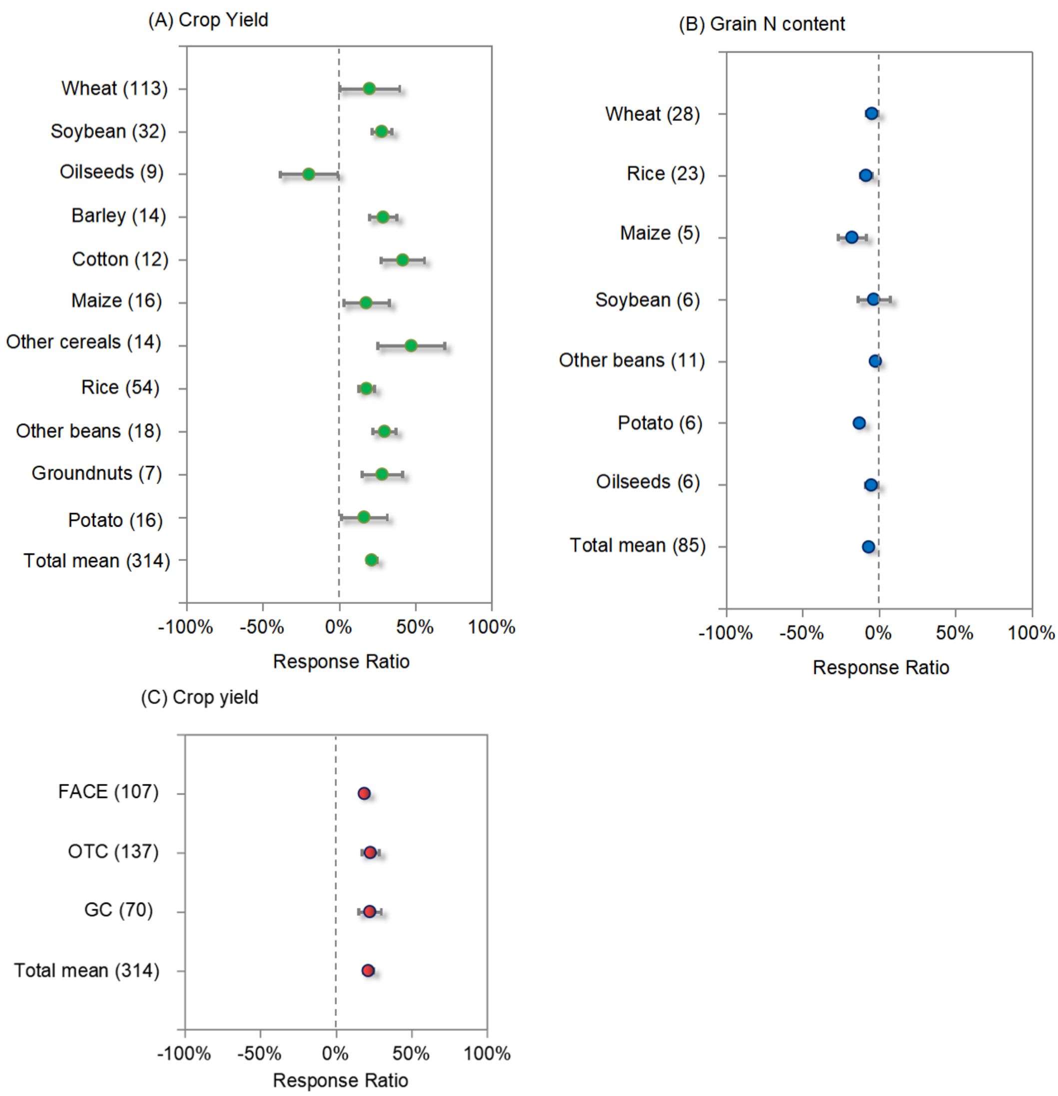

Extended Data Fig. 1 Effects of elevated CO_2 levels on crop yield and grain N content in croplands. (**A**) Crop yield by crop groups; (**B**) Grain N content by crop groups; (**C**) Crop yield by manipulation methods, including FACE (Free-air CO_2 Enrichment Experiment), OTC (Open-top Chamber), and GC (Growth Chamber). The error bars of the mean value indicate 95% confidence interval, and the value is significant if the 95% confidence interval does not overlap zero. The numbers in the parenthesis denote the number of observations in the meta-analysis.

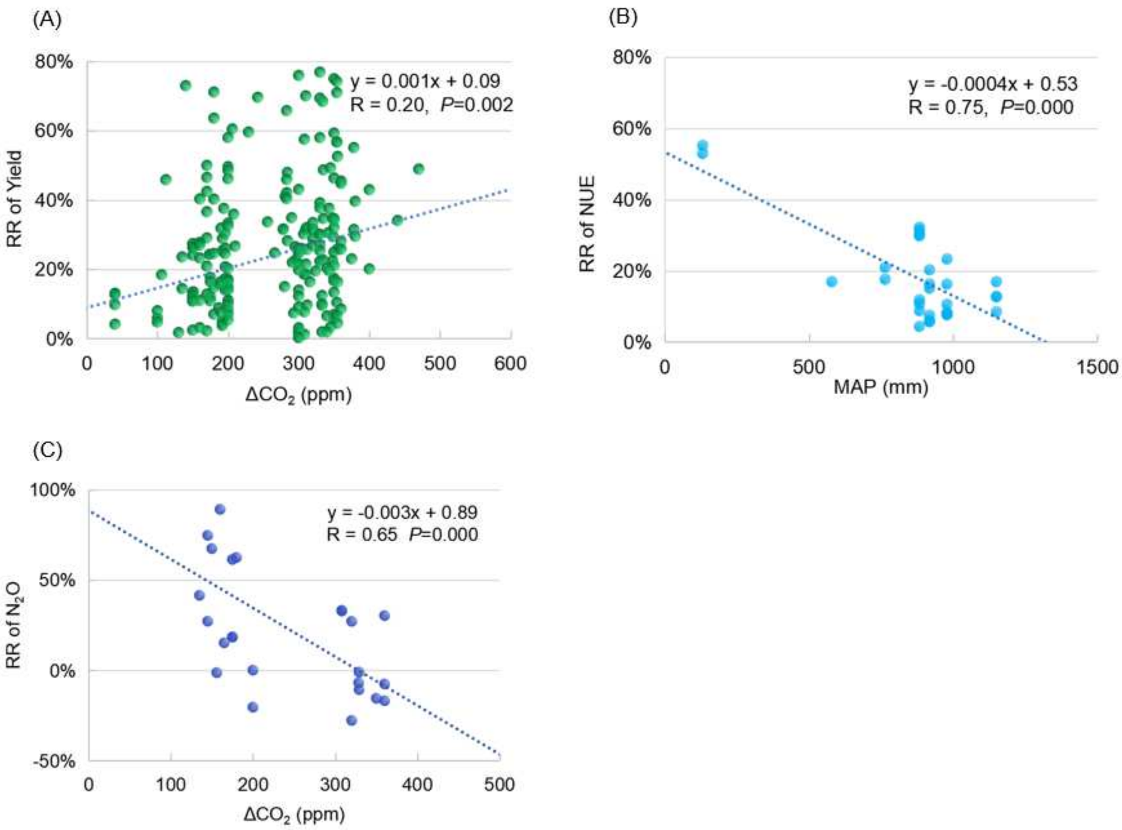

Extended Data Fig. 2 Meta-regressions between response ratios (RR) of variables and environmental factors. (**A**) crop yield versus ΔCO_2 (elevated CO_2 level relative to ambient CO_2); (**B**) NUE versus MAP (mean annual precipitation at the study site); (**C**) N_2O versus ΔCO_2. Unit ppm denotes parts per million.

A

Scenario		Social-economic factor	Climate factor
Baseline scenario	SSP1 (baseline)	Sustainable society	no climate change, fixed CO_2 since 2020
	SSP2 (baseline)	BAU (middle road)	no climate change, fixed CO_2 since 2020
	SSP4 (baseline)	Stratified society	no climate change, fixed CO_2 since 2020
eCO_2 scenario	SSP1-1.9	Sustainable society	Elevated CO_2 to RCP1.9 level
	SSP2-4.5	BAU (middle road)	Elevated CO_2 to RCP4.5 level
	SSP4-6.0	Stratified society	Elevated CO_2 to RCP6.0 level
Manure recycle scenario 1		as a variant of eCO_2 SSP2-4.5 scenario, improving the global manure Nr recycling ratio to 35% by 2050 relative to 30% in the base year 2020	
Manure recycle scenario 2		as a variant of eCO_2 SSP2-4.5 scenario, improving the global manure Nr recycling ratio to 40% by 2050 relative to 30% in the base year 2020	

B

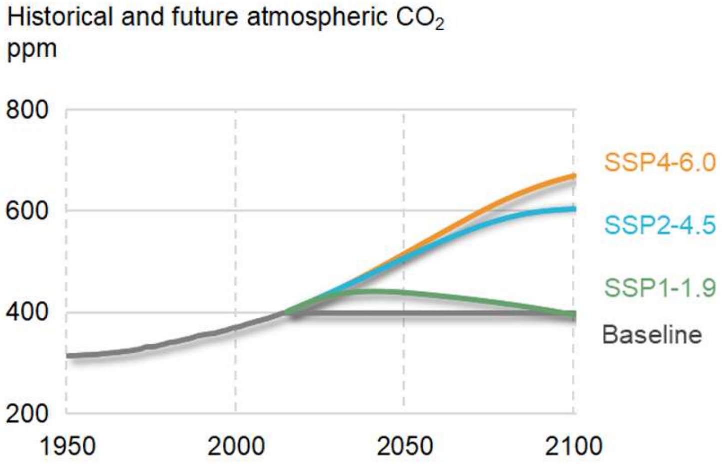

Extended Data Fig. 3 Scenario design of the study. (**A**) Simplified narratives of the scenarios. (**B**) Historical and future atmospheric CO_2 levels in the baseline scenario and elevated CO_2 scenario during 1950-2100.

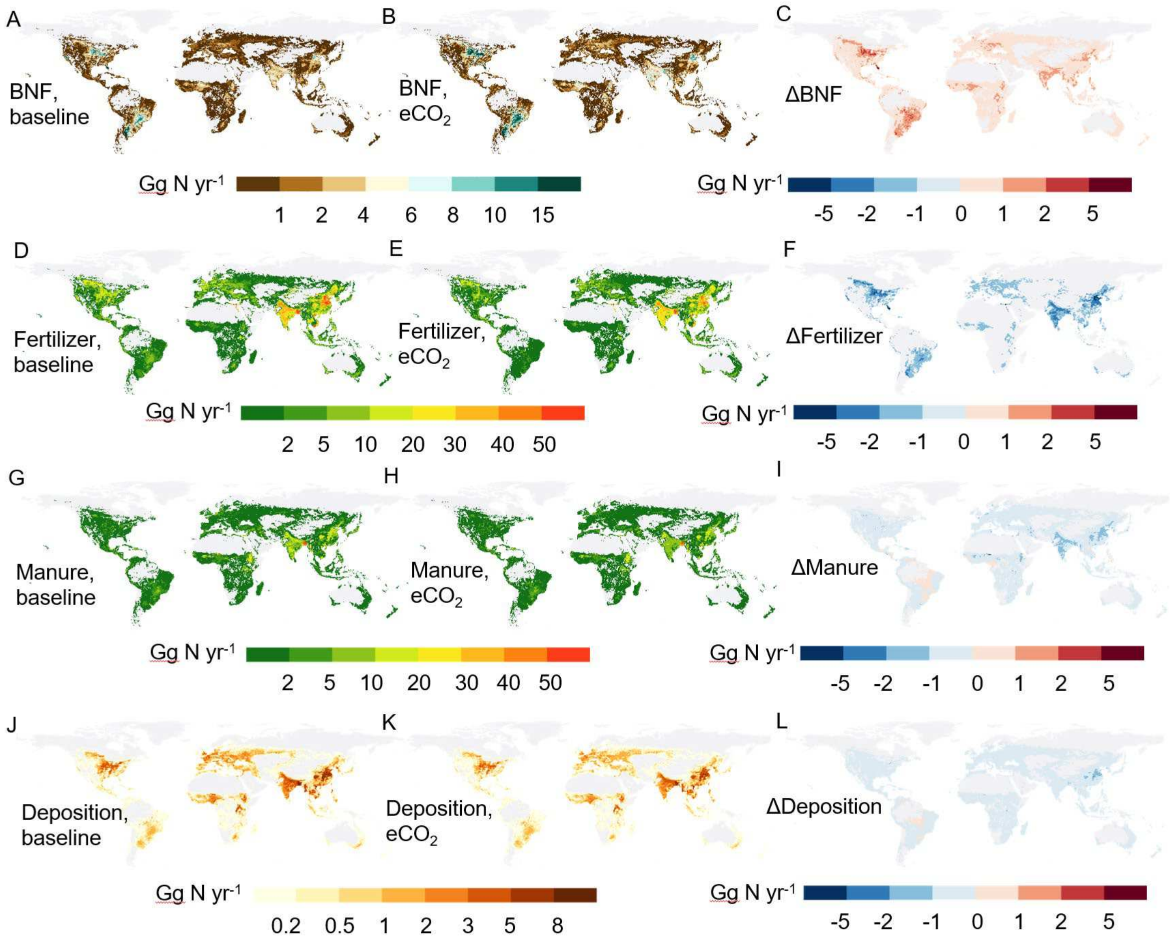

Extended Data Fig. 4 N input of global cropland and their changes under elevated CO_2 scenario (SSP2-4.5) relative to baseline scenario (no climate change) in 2050. Biological N fixation (BNF) in baseline scenario (**A**), eCO_2 scenario (**B**), and *Δ*BNF (**C**); Fertilizer in baseline scenario (**D**), eCO_2 scenario (**E**), and *Δ*Fertilizer (**F**); Manure in baseline scenario (**G**), eCO_2 scenario (**H**), and *Δ*Manure (**I**); Deposition in baseline scenario (**J**), eCO_2 scenario (**K**), and *Δ*Deposition (**L**). Values in the legend reflect the average annual N budget from cropland within a grid cell (0.5 by 0.5 degree). Base map is applied without endorsement from Natural Earth (https://www.naturalearthdata.com/).

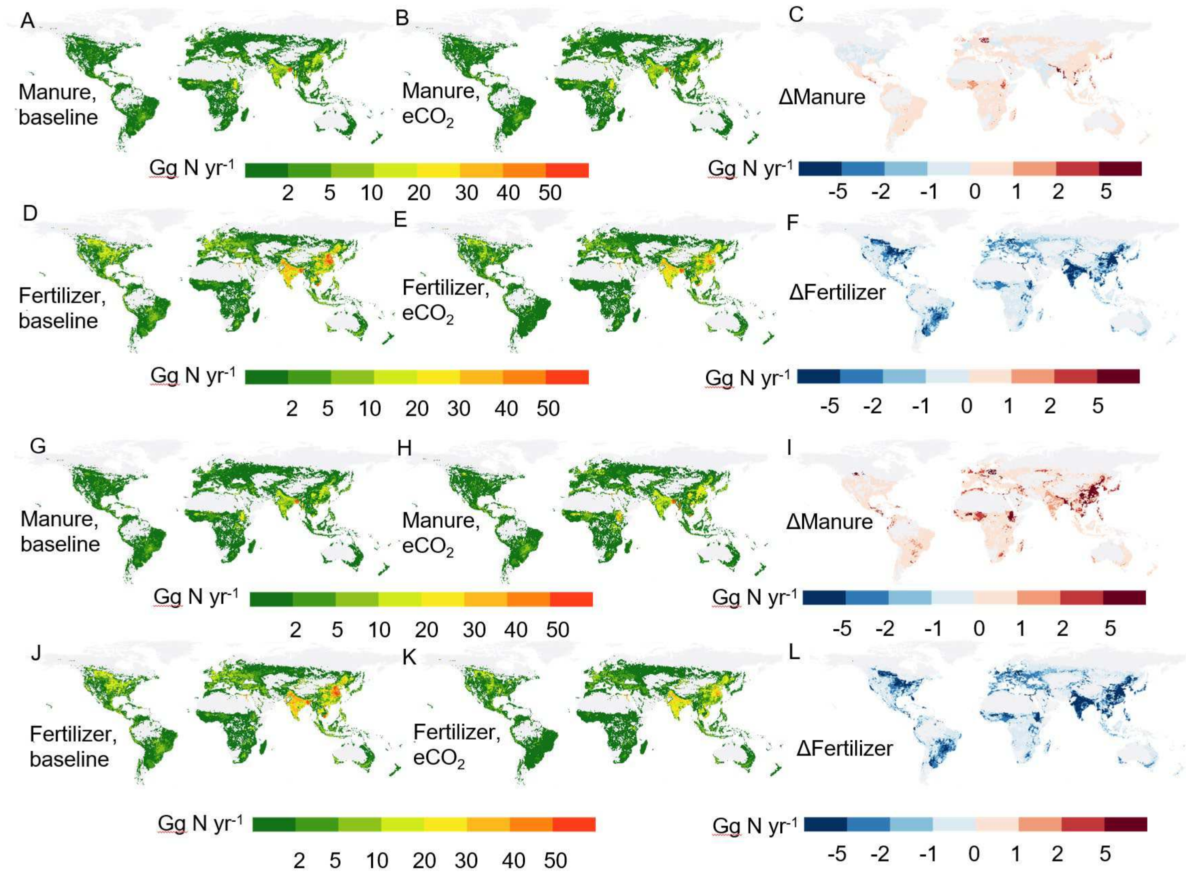

Extended Data Fig. 5 Manure and fertilizer input of global croplands and their changes under supplementary scenario by 2050. (A-F) manure recycle scenario 1 (improving manure recycling ratio to 35%) **(G-L)** manure recycle scenario 2 (improving manure recycling ratio to 40%). Values in the legend reflect the average annual N budget from cropland within a grid cell (0.5 by 0.5 degree).

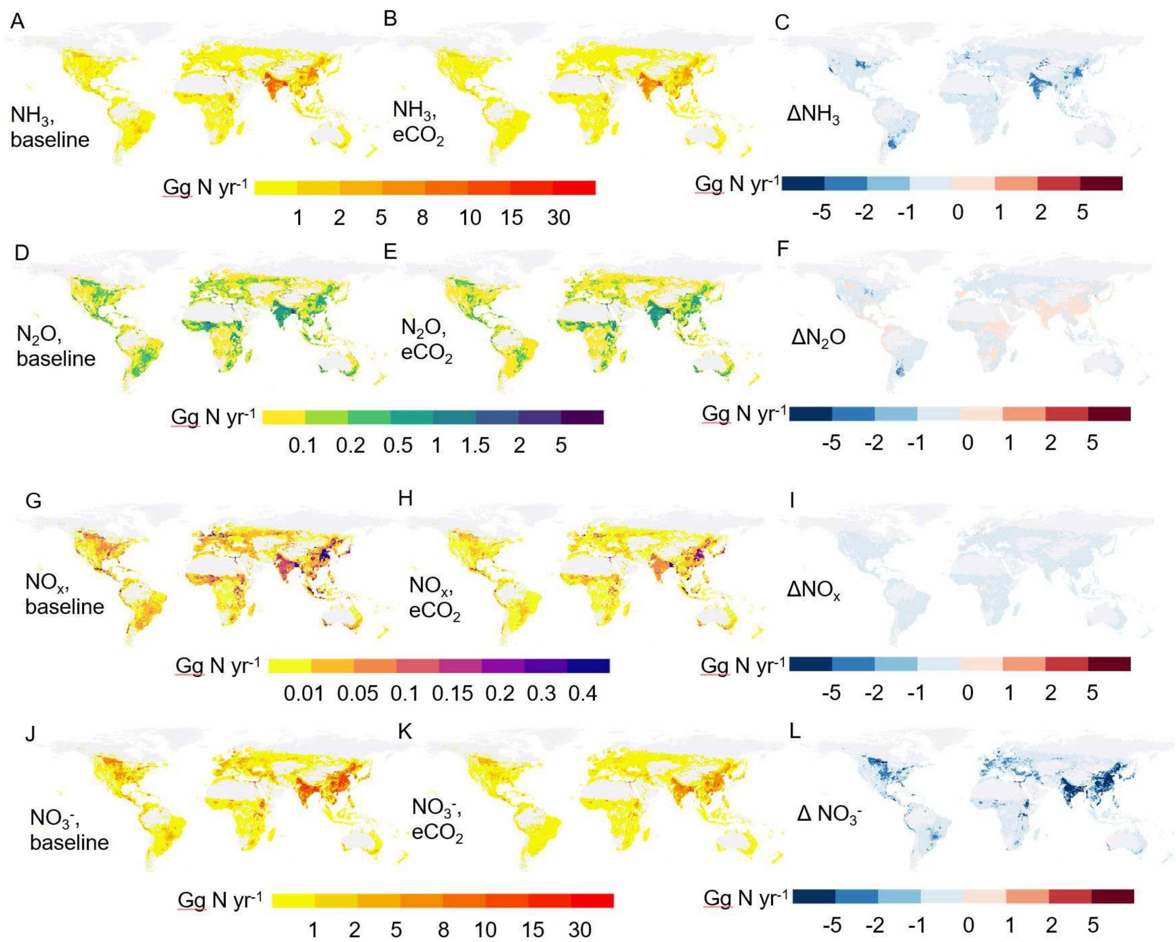

Extended Data Fig. 6 Reactive N loss of global cropland and their changes under elevated CO_2 scenario (SSP2-4.5) relative to baseline scenario (no climate change) in 2050. NH_3 in baseline scenario (**A**), eCO_2 scenario (**B**), and ΔNH_3 (**C**); N_2O in baseline scenario (**D**), eCO_2 scenario (**E**), and ΔN_2O (**F**); NO_x in baseline scenario (**G**), eCO_2 scenario (**H**), and ΔNO_x (**I**); N leaching and runoff in baseline scenario (**J**), eCO_2 scenario (**K**), and ΔN leaching and runoff (**L**). Values in the legend reflect the average annual N budget from cropland within a grid cell (0.5 by 0.5 degree).

Supplementary Files

This is a list of supplementary files associated with this preprint. Click to download.

- SIECO2.pdf